JOURNAL OF VIROLOGY, Sept. 2006, p. 8639–8652 Vol. 80, No. 17
0022-538X/06/$08.00+0 doi:10.1128/JVI.00560-06

Highly Conserved Regions within the Spike Proteins of Human Coronaviruses 229E and NL63 Determine Recognition of Their Respective Cellular Receptors

Heike Hofmann,[1,2,3] Graham Simmons,[4,5] Andrew J. Rennekamp,[4] Chawaree Chaipan,[1,2] Thomas Gramberg,[1,2] Elke Heck,[1,2] Martina Geier,[1,2] Anja Wegele,[1,2] Andrea Marzi,[1,2] Paul Bates,[4] and Stefan Pöhlmann[1,2]*

Institute for Clinical and Molecular Virology[1] and Nikolaus-Fiebiger-Center,[2] University Erlangen-Nürnberg, 91054 Erlangen, Germany; Institute for Infection Medicine, University of Kiel, 24105 Kiel, Germany[3]; Department of Microbiology, University of Pennsylvania, Philadelphia, Pennsylvania[4]; and Blood Systems Research Institute, San Francisco, California 94118[5]

Received 17 March 2006/Accepted 12 June 2006

We have recently demonstrated that the severe acute respiratory syndrome coronavirus (SARS-CoV) receptor angiotensin converting enzyme 2 (ACE2) also mediates cellular entry of the newly discovered human coronavirus (hCoV) NL63. Here, we show that expression of DC-SIGN augments NL63 spike (S)-protein-driven infection of susceptible cells, while only expression of ACE2 but not DC-SIGN is sufficient for entry into nonpermissive cells, indicating that ACE2 fulfills the criteria of a bona fide hCoV-NL63 receptor. As for SARS-CoV, murine ACE2 is used less efficiently by NL63-S for entry than human ACE2. In contrast, several amino acid exchanges in human ACE2 which diminish SARS-S-driven entry do not interfere with NL63-S-mediated infection, suggesting that SARS-S and NL63-S might engage human ACE2 differentially. Moreover, we observed that NL63-S-driven entry was less dependent on a low-pH environment and activity of endosomal proteases compared to infection mediated by SARS-S, further suggesting differences in hCoV-NL63 and SARS-CoV cellular entry. NL63-S does not exhibit significant homology to SARS-S but is highly related to the S-protein of hCoV-229E, which enters target cells by engaging CD13. Employing mutagenic analyses, we found that the N-terminal unique domain in NL63-S, which is absent in 229E-S, does not confer binding to ACE2. In contrast, the highly homologous C-terminal parts of the NL63-S1 and 229E-S1 subunits in conjunction with distinct amino acids in the central regions of these proteins confer recognition of ACE2 and CD13, respectively. Therefore, despite the high homology of these sequences, they likely form sufficiently distinct surfaces, thus determining receptor specificity.

The family *Coronaviridae* comprises enveloped viruses with a single, positive-stranded genomic RNA of approximately 30 kb, which are divided into three groups containing animal and human viruses (30). The human coronaviruses (hCoV) 229E (group I) and OC43 (group II) were identified in the 1960s and have been shown to cause common cold-like symptoms in humans (30). The severe acute respiratory syndrome coronavirus (SARS-CoV) emerged in Asia in 2002 and experienced a global spread in 2003, with 8,096 recorded cases and 774 fatalities (50, 51, 57, 58). SARS-CoV was likely transmitted from palm civets to humans in animal markets (24), while bats might constitute the natural reservoir of the virus (37, 41). Subsequent to the identification of SARS-CoV, two other novel hCoVs were identified, both of which are clearly less pathogenic than SARS-CoV. hCoV-HKU-1 is a novel group II virus associated with community-acquired pneumonia in Hong Kong (66, 67). hCoV-NL63 belongs to group I CoVs (20, 62), is globally distributed, and is associated with both upper and lower respiratory tract infections (1, 4, 35, 47, 60, 61) and with croup (63). Moreover, the New Haven coronavirus (18), which is most likely identical to hCoV-NL63, was reported to be associated with Kawasaki disease (17), although this association has been challenged (11, 53). Thus, several hCoVs cause clinically relevant diseases, and understanding the different facets of their replication strategies is required for the development of vaccines and antiviral compounds.

Entry of SARS-CoV into target cells is driven by interactions of the viral spike (S) protein with the cellular metallopeptidase angiotensin converting enzyme 2 (ACE2) (40), an integral component of the renin angiotensin system (13). Additionally, several cellular lectins augment SARS-S-dependent infection (22, 34, 43, 70). ACE2 was detected on important target cells of SARS-CoV, like pneumocytes and enterocytes in the small intestine (15, 23, 25), and ACE2 expression on cell lines correlates with susceptibility to SARS-S-driven infection (27, 48), strongly indicating that ACE2 engagement plays a key role in SARS-CoV spread. Moreover, SARS-S interactions with ACE2 might directly contribute to the development of SARS (36), since it was shown that soluble ACE2 treatment protects mice from the development of lung disease (33), while disease is exacerbated by SARS-S-mediated down-modulation of ACE2 (36).

The interaction of SARS-S and ACE2 has been characterized on the molecular level by mutagenic analyses (2, 8, 42, 65, 69) and by elucidation of the structure of the SARS-S receptor binding domain bound to ACE2 (38). Notably, several variations in the SARS-S–ACE2 interface, due to species-specific differences in human and rodent ACE2 or in the receptor binding site of SARS-CoV isolated from humans and civet

* Corresponding author. Mailing address: University Erlangen-Nürnberg, Nikolaus-Fiebiger-Center for Molecular Medicine, Glückstraße 6, 91054 Erlangen, Germany. Phone: 49 9131 8529142. Fax: 49 9131 8529111. E-mail: snpoehlm@viro.med.uni-erlangen.de.

cats, were shown to impair the SARS-S interaction with ACE2 and might thus contribute to the species specificity of SARS-CoV (31, 42). For example, the amino acid exchange of K353H in rat ACE2 compared to human ACE2 was demonstrated to prevent appreciable usage of this receptor by SARS-S (42). Likewise, sequence differences between murine and human ACE2 were found to reduce but not abrogate SARS-S interactions with this receptor, which might limit SARS-CoV replication in mice (39).

Inhibition of SARS-S-dependent entry by lysosomotropic agents suggested that the membrane fusion activity of SARS-S is triggered by low pH (28, 55, 70). However, it has recently been demonstrated that blocking of SARS-S-driven entry by neutralization of intracellular pH is due to abrogation of the activity of the pH-dependent cellular cysteine proteases cathepsin B and particularly cathepsin L (32, 54). These proteins are believed to activate SARS-S in cellular endosomes and seem to be essential for SARS-S-driven membrane fusion (32, 54). Thus, cellular entry of SARS-CoV resembles that of reoviruses (3, 16, 21) and filoviruses (10), which also depend on cathepsin activity.

hCoV-NL63 shows high sequence homology to hCoV-229E (52, 62), and it was therefore suspected that both viruses might use the hCoV-229E receptor CD13 (14, 71) for entry into target cells. However, our recent work demonstrated that NL63-S binds to ACE2 and that hCoV-NL63 engages ACE2 for cellular entry (29). Therefore, the comparative analysis of SARS-S and NL63-S interactions with ACE2 might contribute to the understanding of viral pathogenesis and the generation of antivirals. Here, we show that expression of ACE2 but not cellular lectins on nonpermissive cells allows for NL63-S-dependent infection, providing a so-far-missing formal proof that ACE2 is a functional receptor for NL63-S-mediated infection and that most likely a coreceptor is not required for hCoV-NL63 entry. Comparative analysis of human ACE2 variants and murine ACE2 with NL63-S and SARS-S revealed that both S-proteins might engage ACE2 differentially. Moreover, NL63-S-driven cellular entry was less dependent on intracellular low pH and activity of cellular proteases compared to SARS-S-mediated entry, further highlighting that both proteins might differ in their requirements for mediating cellular entry. Finally, extensive mutagenic analyses of NL63-S and 229E-S demonstrated that an N-terminal domain unique to NL63-S is dispensable for ACE2 engagement, while both a central and a C-terminal domain in the S1 units of both S-proteins were found to be required for binding to their cognate cellular receptors.

MATERIALS AND METHODS

Plasmid construction and in vitro mutagenesis. Eukaryotic expression vectors encoding the spike proteins of hCoV-NL63, hCoV-229E, and SARS-CoV as well as the glycoproteins of murine leukemia virus (MLV) and vesicular stomatitis virus (VSV) have been described previously (29, 55). The expression plasmid encoding murine ACE2 was constructed by reverse transcription-PCR of the ACE2 coding region from RNA derived from murine cardiac cells followed by digestion and ligation of the insert with the pCAGGS plasmid (49). Point mutagenesis studies were performed by sequence overlap extension PCRs, resulting in ACE2 mutants K353A, E145/N147/D157A, and Y510A. The amino acid exchange K353H in ACE2 was generated by amplification of the N-terminal sequences using oligonucleotides 5′-CCCGGTACCCACCATGTCAAGCTCTTCCTGGCTCCTTCTC-3′ and 5′-GCACATAAGGATCCTGAAGTCGCCGTGCCCCAGGTCCCAAGCTGTGGG-3′. The resulting PCR product was cloned into the pcDNA3.1zeo-ACE2 plasmid (27) using KpnI and the internal BamHI site. An expression plasmid for human CD13 has been described previously (29). The NL63-S mutant lacking the N-terminal 178 amino acids (aa) (NL63-SΔ unique) was generated by amplification of the N-terminal NL63-S sequences using oligonucleotides 5′-ACTGAATTCACCATGAAACTTTTCTTGATTTTGCTTGTTTTGCCCCTGGCCTCTTGCTTTTTCTATTCCTGTGTTTTTAGTGTTGTCAACGCC-3′ (encoding the NL63-S signal peptide fused amino acids 179 and following in NL63-S) and 5′-AGTGCCACTCTTTAAATAAATGTGC-3′ followed by insertion into pCAGGS-NL63-S via EcoRI and NheI. For expression of soluble spike glycoproteins, the S1 subunit-encoding sequences were fused to the constant part of human immunoglobulin G (IgG) via PCR and cloned in frame with the amino-terminal murine IgG kappa signal peptide in the eukaryotic expression vector pAB61 (5). The expression vector for the soluble S1 unit of the SARS-CoV S-protein has been described previously (29). PCR fragments for generation of NL63-S1 deletion mutants were cloned into the pAB61 plasmid using KpnI and BamHI. A fragment spanning the coding region of amino acids 369 to 560 within 229E-S was amplified using oligonucleotides 5′-AGTCAAGCTTTGCCCTTTTTCTTTTGGC-3′ and 5′-GATCGGATCCAGAACCATCTGCACAAACGCC-3′ and cloned into the pAB61 plasmid via HindIII and BamHI. For construction of chimeric mutants, the respective fragments were amplified by sequence overlap extension PCR using the NL63-S or 229E-S expression plasmids as templates, and the resulting PCR products were ligated with the pAB61 vector. All PCR-amplified sequences were confirmed by automated sequence analysis. Pair-wise amino acid sequence alignments were performed using the blosum62mt2 score matrix with paired cysteine residues (Invitrogen Corp., San Diego, CA).

Cell culture, transfection, infection, and reporter assays. BHK, Huh-7, and 293T cells were propagated in Dulbecco's modified Eagle's medium supplemented with 10% fetal bovine serum (FBS), penicillin, and streptomycin and were grown at 37°C and 5% CO_2. The medium for Huh-7 cells was additionally supplemented with a 1% amino acid cocktail (Invitrogen Corp., San Diego, CA). Lectin-expressing B-THP cells were maintained in RPMI 1640 medium supplemented with 10% FBS, penicillin, and streptomycin (68). Human immunodeficiency virus-based pseudotypes were generated as described elsewhere (28, 29). Briefly, 293T cells were cotransfected by a standard calcium phosphate transfection technique with a viral envelope expression plasmid in combination with the pNL4-3-Luc-R^-E^- plasmid (12, 26). The culture supernatants were harvested 48 h after transfection, passed through 0.4-μm filters, aliquoted, and stored at −80°C. For infection experiments, target cells were seeded onto 96-well plates at a density of 8×10^3 and incubated with equal volumes of viral supernatants normalized for comparable expression of the luciferase reporter gene on permissive Huh-7 cells. Generally, the medium was replaced after 12 h, and luciferase activity was determined 72 h after transduction using a commercially available kit as recommended by the manufacturer (Promega, Madison, WI). For cell-cell fusion assays, two populations of cells were used: 293T effector cells seeded in six-well plates at 3×10^5/well were transfected with either an empty pCAGGS plasmid or a vector encoding the S-protein of hCoV-NL63 or SARS-CoV in combination with plasmid pGAL4-VP16 encoding the herpes simplex virus VP16 transactivator fused to the DNA binding domain of the yeast transcription factor GAL4 (59). In parallel, BHK target cells were seeded in 48-well plates at 3×10^4 and transfected with pcDNA3 or expression vectors for ACE2 variants together with plasmid pGal5-luc, in which luciferase reporter gene expression is controlled by five GAL4 binding sites (59). The day after transfection, effector cells were diluted in fresh medium and added to the target cells. Cell-cell fusion was quantified by determination of luciferase activities in cell lysates 48 h after cocultivation.

Inhibition of infection by protease inhibitors and bafilomycin A1. For inhibition of cellular cysteine proteases, 293T cells were pretreated for 1 h with E64c (Sigma, Taufkirchen, Germany). The medium was removed and replaced with the same inhibitor at double the final concentration. An equal volume of pseudotypes was then added, and cells were spin infected to concentrate particles on the cell surface. After spin infection, the cells were incubated for 5 h, and the medium was replaced with fresh Dulbecco's modified Eagle's medium without drug. Cells were assayed for luciferase activity after 40 h. For neutralization of intracellular pH, Huh-7 cells were preincubated with 50 μl culture medium containing bafilomycin A1 (Sigma, Taufkirchen, Germany) at two times the final concentration for 10 min and then inoculated with 50 μl of infectivity-normalized virus supernatants. After an overnight incubation, the medium was changed and luciferase activities in cell lysates were determined 3 days after infection.

Binding of soluble glycoproteins to receptor-positive cells. To obtain soluble hCoV-NL63–, hCoV-229E–, or SARS-CoV-S1–IgG fusions, 293T cells were transfected with the respective expression vectors. Plasmid pAB61 encoding only IgG was used as a control. Two days after transfection, the supernatants containing the fusion

proteins were concentrated using Centricon Plus-20 centrifugal filters (Millipore, Schwalbach, Germany), aliquoted, and stored at −80°C. The respective IgG fusion proteins were separated by 6 or 10% sodium dodecyl sulfate-polyacrylamide gel electrophoresis, analyzed by Western blotting using an anti-human IgG–horseradish peroxidase conjugate (Dianova, Hamburg, Germany), and detected using the Super-Signal West Pico chemiluminescence substrate (PerbioScience, Bonn, Germany). Comparable protein amounts were thereafter used for binding to receptor-positive cells. Receptor-positive cells were obtained by transfection of 293T cells with either an empty pcDNA3 vector or expression plasmids encoding human CD13 or ACE2. In each experiment, the cells transfected with a defined receptor were pooled to ensure that all target cells expressed identical receptor levels at their surface. Alternatively, B-THP control cells or B-THP cells stably expressing DC-SIGN and DC-SIGNR were employed. Soluble IgG fusion proteins in a total volume of 100 μl fluorescence-activated cell sorting (FACS) buffer (phosphate-buffered saline with 3% FBS) were added to the cells for 30 min on ice. After washing, the cells were incubated with anti-human Cy5-coupled secondary antibodies (Dianova, Hamburg, Germany) at a final concentration of 15 μg/ml for 30 min on ice, and binding was determined by flow cytometry using a FACSCalibur flow cytometer (Becton Dickinson).

RESULTS

ACE2, but not DC-SIGN and DC-SIGNR, functions as a receptor for NL63-S-mediated infection on nonpermissive cells. We and others have previously shown that the SARS-CoV receptor ACE2 of human origin (hACE2) can be used by hCoV-NL63 for infectious entry (29; M. K. Smith, S. Tusell, E. A. Travanty, B. Berkhout, L. van der Hoek, and K. V. Holmes, Xth Int. Nidovirus Symp., Colorado Springs, Colo., poster P5-6, 2005); however, these experiments were performed on 293T and Huh-7 cells, which endogenously express hACE2 and are permissive to SARS-S- and NL63-S-driven infections (27, 40, 48, 64). In order to investigate if expression of hACE2 on nonpermissive cells allows for NL63-S-mediated infection or whether a coreceptor might be required, we transiently expressed hACE2 on nonpermissive BHK cells followed by infection with SARS-S- and NL63-S-bearing pseudotypes and control pseudoparticles bearing the G-protein of VSV (VSV-G) normalized for comparable infectivity on 293T cells (Fig. 1A, left panel). Control transfected BHK cells were efficiently infected by VSV-G pseudotypes but were refractory to infection by reporter viruses carrying the S-proteins of SARS-CoV and hCoV-NL63, for which reporter gene activities in the background range were measured (Fig. 1A and data not shown). However, the presence of hACE2 rendered these cells highly susceptible to infection mediated by both S-proteins, whereas reporter gene activity in VSV-G-infected cells remained constant (Fig. 1A, right panel). Comparable results were obtained when the experiment was performed on nonpermissive HeLa cells, albeit the overall infection efficiency was reduced (data not shown). This suggests that as for SARS-CoV, hACE2 serves as a functional receptor for hCoV-NL63, with hACE2 expression being sufficient for entry into otherwise-nonpermissive cells.

Since conflicting data concerning a potential role of DC-SIGN and the related protein DC-SIGNR (collectively referred to as DC-SIGN/R) as a SARS-CoV receptor have been documented (34, 43, 70), we sought to analyze a role of these lectins in NL63-S-mediated entry. For this, we transfected BHK cells with expression plasmids for DC-SIGN/R either alone or in combination with hACE2 (Fig. 1B). Again, no difference in infectivity was noted when cells were incubated with particles bearing VSV-G. In accordance with our previous data (43), neither lectin alone mediated SARS-S infection, but coexpression of hACE2 resulted in an enhancement of infection of approximately fivefold (Fig. 1B). Similarly, lectin expression did not render the cells permissive for NL63-S-mediated entry but repeatedly enhanced entry of NL63-S pseudotypes in the presence of hACE2 (approximately twofold) (Fig. 1B), albeit less efficiently than SARS-S-dependent entry. Therefore, we analyzed whether NL63-S differed in its ability to bind these lectins compared to SARS-S. However, by employing FACS-based binding assays using soluble NL63-S or SARS-S fused to IgG and B-THP cells stably expressing DC-SIGN/R, no appreciable difference in lectin binding was detected (Fig. 1C). In summary, NL63-S-mediated infectious entry is dependent on the presence of hACE2 on nonpermissive cells, and coexpression of DC-SIGN/R slightly augments NL63-S-driven infection.

Evidence that NL63-S and SARS-S engage hACE2 differentially. For SARS-CoV, it was shown that the murine ACE2 homologue (mACE2) cannot be used efficiently as a receptor (39); furthermore, amino acid 353 within hACE2 (mutant K353H) has been identified as important for the interaction with SARS-S (42). In order to more closely analyze the role of hACE2 as a receptor for hCoV-NL63, 42 different hACE2 point mutants including the K353H variant were generated and analyzed for their ability to mediate NL63-S and SARS-S entry in parallel. No difference in comparison with wild-type hACE2 was observed for most of the point mutants in pseudotype infection assays using the respective S-proteins (data not shown). The only exceptions were the triple mutant E145/N147/D157A and the mutants Y510A and K353H, the latter being in accordance with published data (42). These variants were examined more closely in the following experiments. Murine ACE2, hACE2 wild type, and the hACE2 mutants mentioned above were transiently expressed on nonpermissive BHK cells. BHK cells were chosen, since we wanted to exclude that endogenous hACE2 on, for example, 293T cells modulates the results obtained for the ACE2 variants. Moreover, transiently transfected BHK cells express lower amounts of hACE2 compared to the widely used 293T cells (data not shown) and might therefore be particularly suitable for uncovering differences in hACE2 usage, taking into account that overexpression of the receptor might mask differences in usage of receptor variants (39). First, we investigated if all variants were expressed on the cell surface of BHK cells at comparable levels (Fig. 2A). While expression of all variants was readily detectable, expression of hACE2 variants harboring amino acid exchanges was somewhat reduced compared to expression of wild-type hACE2. Subsequently, we infected BHK cells expressing these ACE2 mutants with pseudotypes bearing either VSV-G or the S-proteins of hCoV-NL63 and SARS-CoV (Fig. 2B). Reporter gene activities in cells infected with VSV-G particles were independent of the cotransfected ACE2 variants. In agreement with published results (39, 42), mACE2 allowed for less efficient SARS-S entry than the human homologue and SARS-S-mediated infection was less robust on cells expressing the K353H variant (Fig. 2B). Also, variant E145/N147/D157A could not serve as an efficient receptor for SARS-S-bearing particles, while exchange Y510A consistently augmented infectious entry at least twofold (Fig. 2B). In stark contrast to the results obtained with SARS-S-bearing reporter viruses, none of the amino acid exchanges in hACE2 modu-

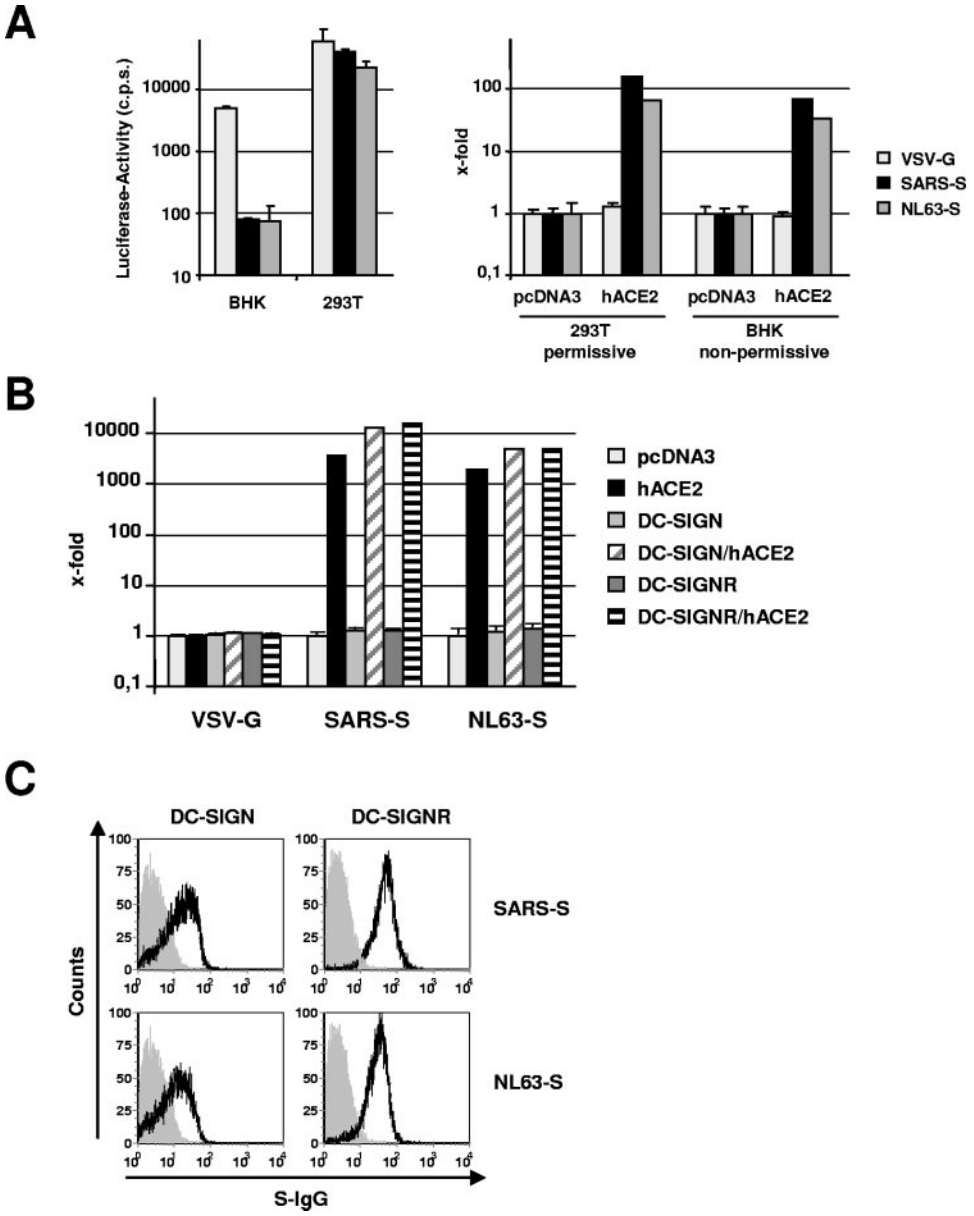

FIG. 1. Expression of hACE2 but not DC-SIGN/DC-SIGNR renders otherwise-nonpermissive cells susceptible to NL63-S-dependent infection. (A) Expression of hACE2 renders otherwise-nonpermissive BHK cells susceptible to NL63-S-driven infection. Permissive 293T and nonpermissive BHK cells were transfected either with pcDNA3 or hACE2 in parallel and infected with infectivity-normalized pseudotypes bearing SARS-S or NL63-S (right panel). Normalization of input virus on 293T cells is shown in the left panel. Luciferase activities were determined 72 h postinfection, and fold activation was calculated based on the infectivity of the respective pseudotypes on target cells transfected with pcDNA3, which was set as 1. Error bars indicate standard deviations (SD). The results of a representative experiment carried out in quadruplicate is shown, and comparable results were obtained in an additional experiment using an independent virus preparation. (B) BHK cells were transfected with pcDNA3, hACE2, or the lectins DC-SIGN and DC-SIGNR or were cotransfected with hACE2 and DC-SIGN or DC-SIGNR. The amount of transfected DNA was kept constant by adding pcDNA3 plasmid. The cells were infected with pseudotypes bearing either VSV-G or the S-proteins normalized for comparable infectivity on Huh-7 cells in quadruplicate, and luciferase activities were determined 72 h postinfection. Fold activation is based on the infectivity on pcDNA3-transfected cells, which was set as 1. A representative experiment is shown and reflects the results of two independent experiments. Error bars indicate SD. (C) Soluble IgG protein (filled histograms) or IgG fusions with either NL63-S or SARS-S were incubated with B-THP cells stably expressing the lectins DC-SIGN and DC-SIGNR as indicated. Bound proteins were detected by FACS using a Cy5-coupled secondary antibody. An independent experiment yielded comparable results.

lated infection driven by NL63-S while, similarly as for SARS-S, NL63-S-dependent entry into mACE2-expressing cells was reduced compared to infection of cells expressing hACE2 (Fig. 2B).

In order to confirm these results in an independent experimental system, we performed cell-cell fusion assays. For this, 293T effector cells were cotransfected with the indicated S-expression vectors and a plasmid encoding the herpes simplex

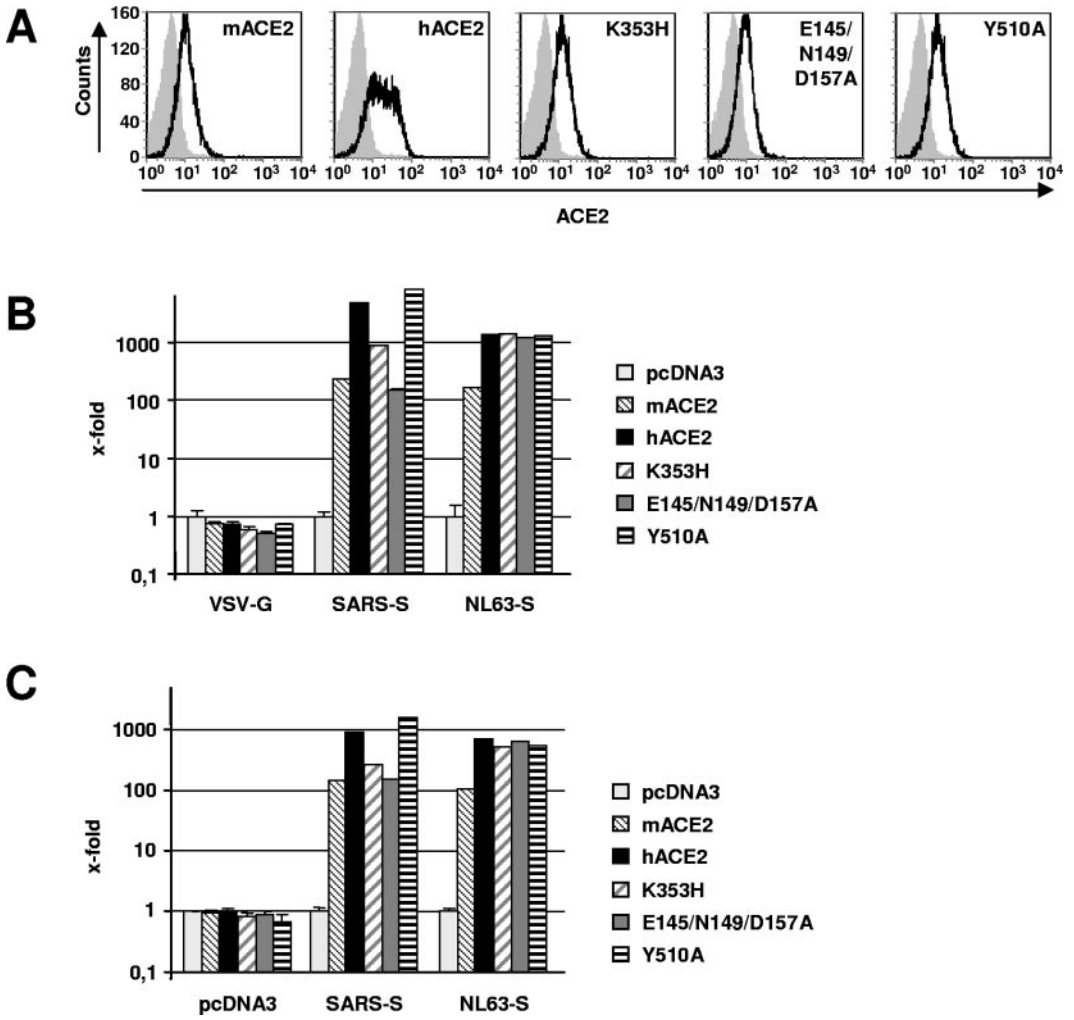

FIG. 2. Analysis of SARS-S and NL63-S engagement of ACE2 variants expressed on nonpermissive BHK cells. (A) BHK cells expressing either mACE2, hACE2, or the indicated hACE2 mutants were stained with a goat-anti-ACE2 polyclonal antiserum and a Cy5-coupled secondary antibody. Filled histograms indicate staining of cells transfected with a control vector, while black lines indicate staining of ACE2-expressing cells. (B) BHK cells were transfected with ACE2 variants as for panel A and overinfected in quadruplicate with pseudotypes bearing VSV-G, SARS-S, or NL63-S. The pseudotypes had previously been normalized for comparable infectivity on Huh-7 cells. Luciferase activities were determined 72 h postinfection. Fold activation is based on the reporter gene activity in cells expressing pcDNA3. The data were confirmed in three additional experiments with independent pseudoparticle preparations. Error bars indicate standard deviations (SD). (C) BHK cells transfected with ACE2 variants as for panel A in combination with plasmid pGal5-luc were used as target cells for fusion with 293T effector cells carrying the S-proteins of SARS-CoV or hCoV-NL63 together with plasmid pGAL4-VP16 as indicated. Cells transfected with pcDNA3/pGAL4-VP16 served as a control. Fold activation was calculated based on the fusion activity (approximately 100 relative light units) of pcDNA3/pGal5-luc-transfected target with pcDNA3/pGAL4-VP16-transfected effector cells, which was set as 1. Each experiment was performed in triplicate. Error bars indicate SD. An independent experiment yielded similar results.

virus transactivator VP16 fused to the DNA binding domain of the yeast transcription factor GAL4 (59). BHK cells transfected with the ACE2 variants and a reporter plasmid, in which expression of luciferase is controlled by five GAL4 binding sites (59), served as target cells. Upon fusion of effector and target cells, expression of the reporter gene is activated. As demonstrated in Fig. 2C, the mutations K353H and E145/N147/D157A reduced SARS-S-dependent cell-cell fusion, while the mutation Y510A slightly increased SARS-S-dependent fusion. In contrast, none of the mutations affected fusion driven by the NL63-S proteins, whereas both NL63-S- and SARS-S-dependent fusion with mACE2-expressing target cells was reduced compared to fusion with cells producing hACE2 (Fig. 2C). Therefore, these data confirm the results obtained with S-bearing pseudotypes and indicate that NL63-S and SARS-S might contact hACE2 differently.

Requirements for hCoV-NL63 S-mediated membrane fusion. Enveloped viruses can enter cells by fusion with the plasma membrane or by receptor-mediated endocytosis into endosomal vesicles and subsequent fusion with an intracellular membrane. In the latter case, acidification of the endosome triggers the fusion activity of the viral glycoprotein (56). For SARS-CoV, this endosomal route of entry is used (28, 55, 70). However, the low pH of the endosome does not directly trigger S-driven membrane fusion but is required for the activity of cellular endoproteases such as cathepsin L, which cleaves

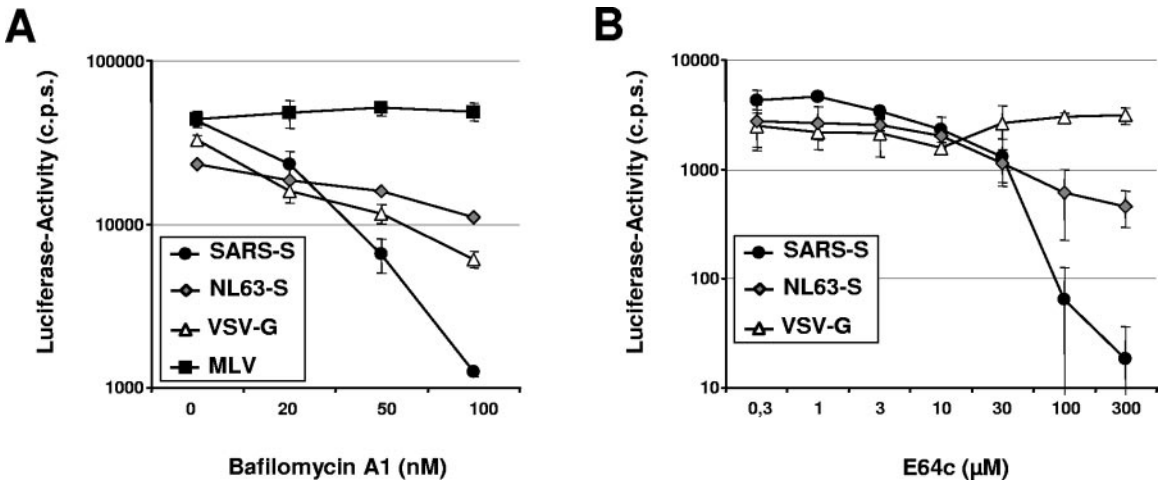

FIG. 3. NL63-S exhibits a reduced dependence on low pH and protease cleavage compared to SARS-S. (A) Huh-7 cells were preincubated with the indicated concentrations of bafilomycin A1 followed by infection with pseudotypes carrying the envelope proteins of MLV, VSV, hCoV-NL63, and SARS-CoV. An experiment performed in quadruplicate is shown, which is representative for a total of three experiments performed with two independent pseudotype preparations. Error bars indicate standard deviations (SD). (B) 293T cells were preincubated with E64c followed by infection with pseudotypes carrying the glycoproteins of VSV, SARS-CoV, and hCoV-NL63 as indicated. Each experiment was performed in quadruplicate; similar results were obtained in an independent experiment. Error bars indicate SD.

SARS-S and thereby triggers S-driven membrane fusion (54). We therefore asked if a low-pH environment is also required for NL63-S-mediated membrane fusion. This was analyzed by preincubation of Huh-7 target cells with serial dilutions of bafilomycin A1 (Fig. 3A), a potent inhibitor of lysosomal acidification. The cells were subsequently pulsed with infectivity-normalized pseudotypes carrying the S-proteins of hCoV-NL63 and SARS-CoV. Pseudotypes bearing the VSV-G protein and the MLV glycoprotein were used as controls, since MLV fuses at neutral pH at the cellular membrane and thus is not affected by inhibitors of endosomal acidification (45, 46), while fusion mediated by VSV-G occurs in intracellular vesicles and depends on low pH (44). Entry driven by VSV-G, hCoV-NL63-S, and SARS-CoV-S was blocked by bafilomycin A1 (Fig. 3A), albeit with different efficiencies. Thus, while bafilomycin A1 reduced VSV-G- and SARS-S-driven entry by 80% and 97%, respectively, NL63-S-dependent infection was only diminished about 50%, indicating that NL63-S-dependent entry might be less dependent on low pH than SARS-S-driven infection. Next, we asked if the differential requirement of SARS-S- and NL63-S-driven infection for low pH might be due to a differential dependence on cleavage by cellular proteases, since cathepsin-mediated, pH-dependent cleavage of S was shown to be essential for SARS-CoV cellular entry (54). To this end, 293T cells were preincubated with the cysteine protease inhibitor E64c for 1 h and overinfected with infectivity-normalized pseudotypes carrying VSV-G or the S-proteins of SARS-CoV and hCoV-NL63 (Fig. 3B). In agreement with published data (54), SARS-S- but not VSV-G-mediated entry was efficiently blocked by E64c (Fig. 3B). A similar observation was made for NL63-S. However, at the highest concentration of inhibitor, infection by SARS-S pseudotypes was more than 50-fold reduced, while NL63-S-dependent entry was only about 7-fold reduced (Fig. 3B). A similar observation was made by Huang and colleagues, who also found that replication-competent hCoV-NL63 was less sensitive to cathepsin inhibitors or inhibitors of lysosomal acidification than SARS-CoV (32). These data suggest that while hCoV-NL63 and SARS-CoV share their receptor and likely the route of entry into the target cells, NL63-S-driven entry exhibits a less pronounced requirement for a low-pH environment and for protease-mediated S-protein cleavage compared to SARS-S.

The unique domain in NL63-S is not required for binding to hACE2. We next sought to identify domains in NL63-S that are involved in binding to ACE2. While NL63-S shares no appreciable sequence identity with SARS-S (20.2%), the NL63-S sequence is 54.6% identical to that of the S-protein of hCoV-229, which engages CD13 for cellular entry (14, 71). Therefore, we reasoned that analysis of chimeric S-proteins should allow identification of regions in NL63-S and 229E-S involved in the engagement of their respective cellular receptors. The fact that NL63-S and 229E-S share high sequence homology but differ in receptor specificity suggests that regions that are not conserved between both proteins might contribute to the interaction with the cognate receptors. As NL63-S harbors a unique domain of 178 amino acids at its N terminus, which is not present in 229E-S (62), we first addressed whether this region might contribute to the interaction with hACE2. For this, we generated soluble fusion proteins consisting of the S1 subunits of 229E-S and NL63-S and variants thereof linked to the Fc portion of human immunoglobulin and assessed binding of these proteins to receptor-expressing cells. Specifically, we fused the unique domain of NL63-S to human IgG (mutant NL63-S aa16-178), deleted the unique domain in NL63-S (mutant NL63-SΔ unique), or fused the unique domain to the S1 subunit of hCoV-229E-S (mutant unique/229E-S). All mutants were concentrated from the supernatants of transiently transfected 293T cells, normalized for comparable protein content by Western blotting, and analyzed for interaction with hACE2 or CD13 using a FACS-based binding assay (Fig. 4A; see also Fig. 5B and 7B for normalization of input proteins). The unique domain alone did not show any receptor binding, indi-

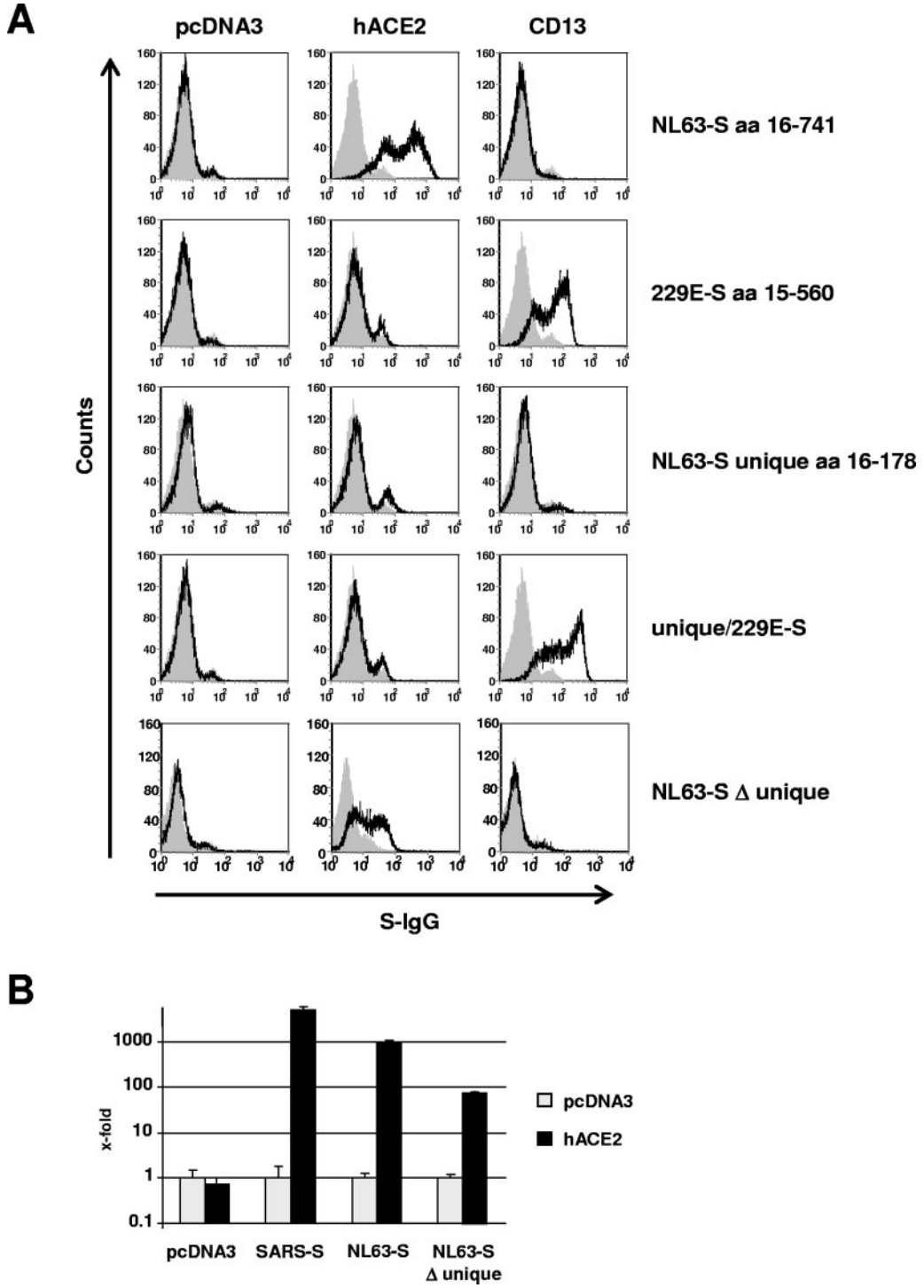

FIG. 4. The unique domain in NL63-S is dispensable for binding to hACE2. (A) 293T cells transfected with either pcDNA3, hACE2, or CD13 were incubated with comparable amounts (as judged by Western blot analyses) of soluble IgG (filled histograms) or IgG fusions of NL63-S wild type (aa 16 to 741; panel 1), 229E-S wild type (aa 15 to 560; panel 2), the NL63-S unique domain (aa 16 to 178; panel 3) alone or fused to 229E-S (panel 4) and NL63-S lacking the unique domain (panel 5; black histograms). Bound proteins were detected by a Cy5-coupled anti-human secondary antibody, and binding was analyzed by FACS. Similar results were obtained in an independent experiment with a different batch of soluble IgG fusion proteins. (B) 293T cells expressing either pcDNA3, SARS-S, NL63-S, or an NL63-S variant lacking the unique domain (NL63-SΔ unique) were fused to cells expressing either pcDNA3 (gray) or hACE2 (black) as described in the legend for Fig. 2C. Fold fusion activity was calculated based on the activity of pcDNA3-transfected cells, which was set as 1. A representative experiment performed in triplicate is shown, and four independent experiments yielded comparable results. Error bars indicate standard deviations.

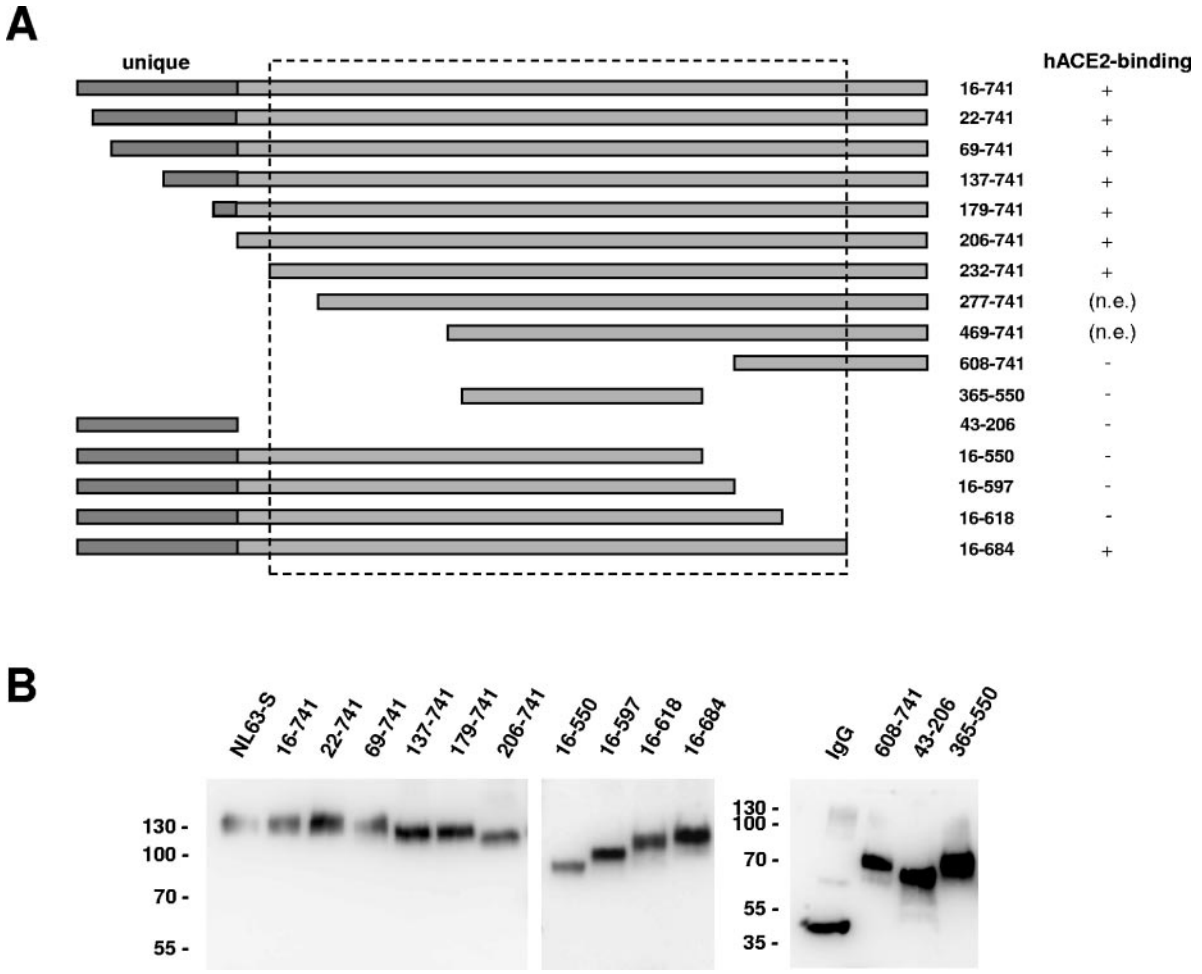

FIG. 5. Schematic representation of NL63-S deletion variants and their interaction with hACE2. (A) The indicated NL63-S deletion mutants (amino acid positions are indicated relative to wild-type NL63-S) were expressed as IgG fusion proteins and analyzed for hACE2 interaction by FACS, as described in the legend to Fig. 4. The data are representative for two independent experiments performed with separate preparations of soluble S-proteins. +, hACE2 binding observed; −, no hACE2 interaction; n.e., respective mutants were not expressed in sufficient amounts. (B) The indicated NL63-S deletion mutants were expressed in 293T cells, concentrated from the supernatant, separated by 6% (left and middle panel) or 10% sodium dodecyl sulfate-polyacrylamide gel electrophoresis (right panel), and normalized for comparable protein amounts by Western blotting prior to the FACS-binding assays.

cating that it does not serve as an independent hACE2 interaction domain (panel 3). Furthermore, the unique/229E-S mutant did not engage hACE2 and bound to CD13 as efficiently as the wild-type protein, indicating that the unique domain does not mask the CD13 recognition motif in 229E-S (panel 4). Also, the deletion of the unique domain from NL63-S did not abrogate hACE2 binding (panel 5), indicating that the unique domain is unlikely to have an important role in NL63-S binding to hACE2. In order to analyze whether the unique domain would be required for NL63-S-mediated membrane fusion, we deleted the unique domain from the full-length protein and performed cell-cell fusion experiments on cells transiently expressing either pcDNA3 or hACE2 (Fig. 4B). The removal of the unique domain was compatible with robust ACE2-dependent membrane fusion, which repeatedly was at least 2 logs over background, albeit less efficient than fusion driven by the wild-type protein. In summary, these data suggest that the N-terminal 178 amino acids from NL63-S are dispensable for receptor binding and membrane fusion. Thus, amino acids in regions highly conserved between NL63-S and 229E-S seem to confer specificity for the interaction with hACE2 and CD13, respectively.

Analysis of NL63-S deletion mutants and chimeric NL63-229E S variants. In order to map the hACE2 binding domain in NL63-S, we first generated a set of N- and C-terminal deletion mutants fused to IgG (Fig. 5A), normalized them for comparable protein content (Fig. 5B), and analyzed binding to 293T cells expressing hACE2 or CD13. None of the NL63-S mutants tested bound to CD13 (data not shown), indicating that no region in NL63-S masks a structure sufficient for interaction with CD13. S-protein variants with deletions of the N-terminal 231 or the C-terminal 57 amino acids bound to hACE2 with similar efficiency as wild-type NL63-S (Fig. 5A), indicating that amino acids 232 to 684 are involved in ACE2 binding. Unfortunately, however, we were not able to further narrow down N-terminal sequences involved in hACE2 inter-

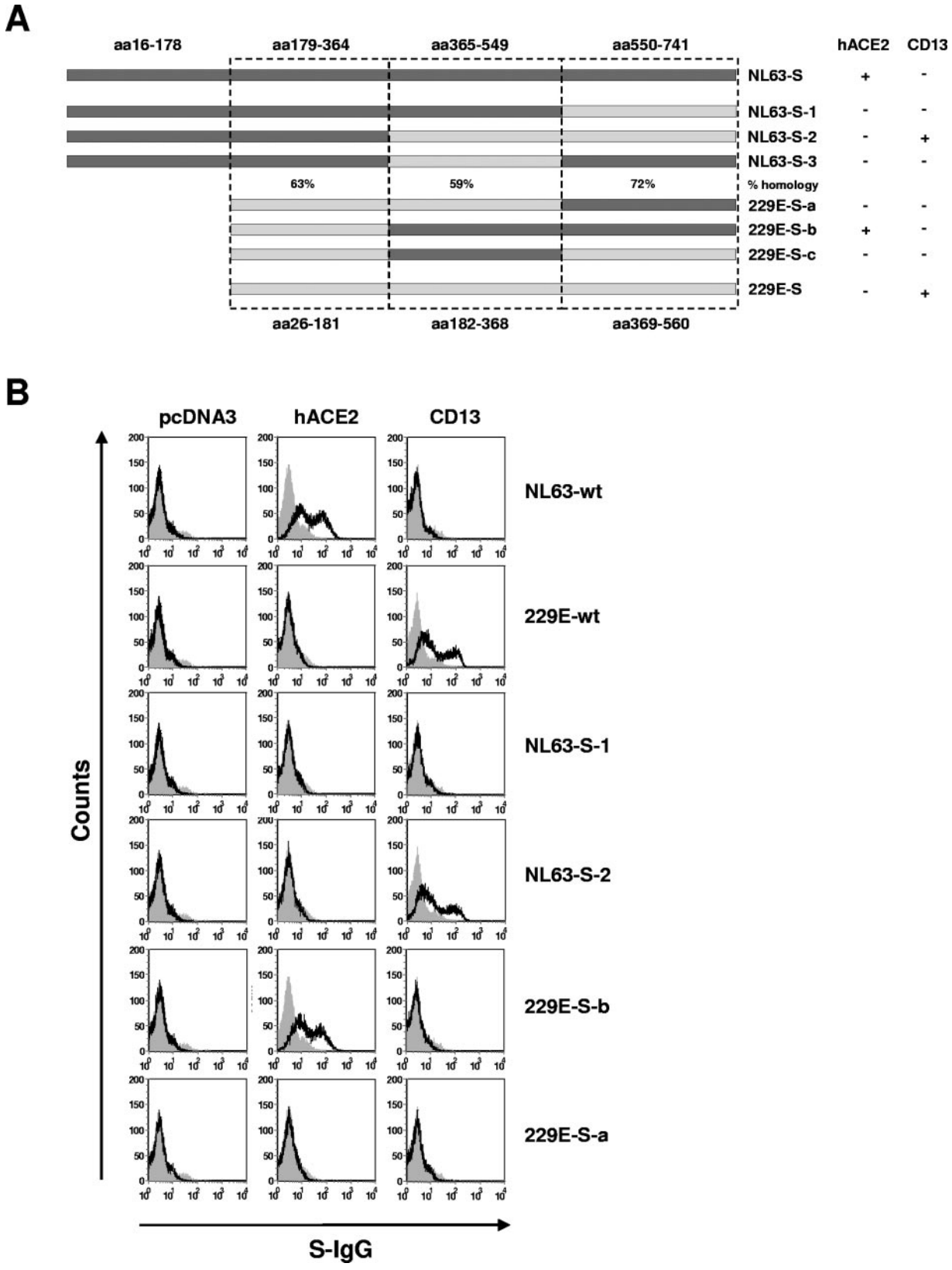

FIG. 6. Binding of S-protein chimeras to hACE2 and CD13. (A) Overview depicting chimeras between NL63-S (dark gray) and 229E-S (light gray) and their interaction with hACE2 and CD13. The percent amino acid homology between the respective subdomains in both proteins is shown; the underlying amino acid residues are indicated. The data are representative of two independent experiments. +, hACE2 binding observed; −, no hACE2 interaction. (B) Representative experiment demonstrating binding of a panel of S-protein chimeras (depicted in panel A) to hACE2 and CD13. 293T cells were transfected with either pcDNA3, hACE2, or CD13, incubated with comparable amounts of soluble IgG (filled histograms) or the indicated IgG fusions (black histograms) (for nomenclature see panel A), and stained with a Cy5-coupled secondary antibody.

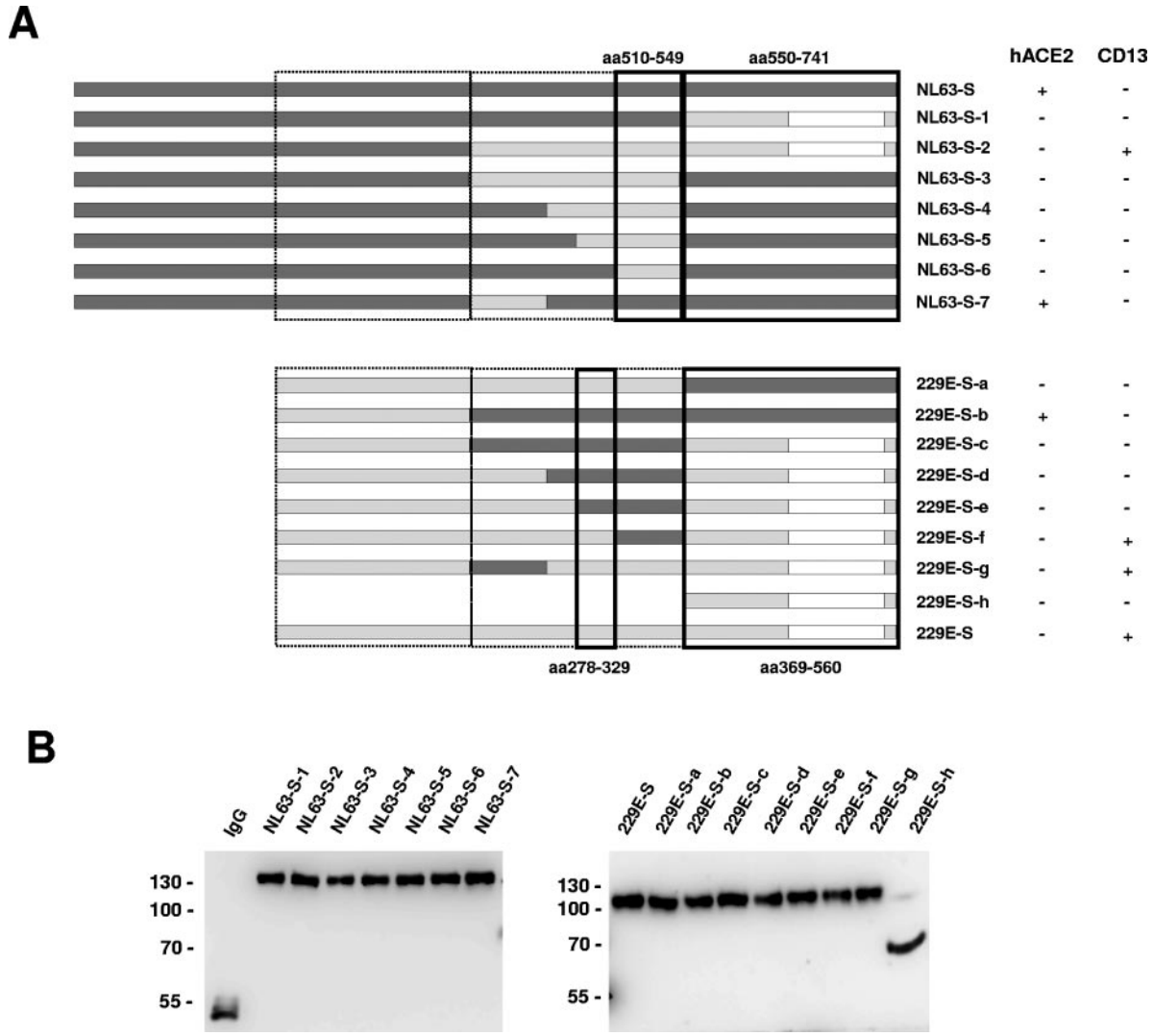

FIG. 7. Identification of domains involved in the receptor interaction of NL63-S and 229E-S. (A) Schematic representation of NL63-S and 229E-S wild type and all analyzed chimeras and their ability to bind hACE2 or CD13, respectively. The deletion mutant 229E-S-h containing only the C-terminal CD13 interaction domain as determined by Bonavia et al. and Breslin et al. (6, 7) was also included. All chimeras were expressed as IgG fusion proteins and analyzed for receptor binding as described in the legend of Fig. 6. Each chimera was tested at least two times in independent experiments. +, interaction with hACE2 or CD13; −, no binding. The domains within NL63-S and 229E-S required for interaction with their receptors are shown by boxes. (B) The indicated chimeras fused to IgG were normalized for comparable protein amounts by Western blotting prior to the FACS-binding experiments.

actions, as all mutants lacking more than the 232 N-terminal amino acids were not expressed to appreciable amounts and could therefore not be analyzed.

As mentioned above, the NL63-S sequences required for hACE2 binding are highly related to those of hCoV-229E-S but still allow for recognition of specific receptors. Therefore, we asked whether a stepwise replacement of domains between both S-proteins would modulate receptor usage. For this, we subdivided the homologous regions between NL63-S and 229E-S into an N-terminal, a central, and a C-terminal domain (Fig. 6A) and constructed chimeric S-proteins containing defined domains of NL63-S fused to the corresponding sequences of 229E-S. All chimeras were efficiently expressed (Fig. 7B) and were therefore used for determination of CD13 and hACE2 binding in parallel. Robust interaction of NL63-S chimera 2 with CD13 was detected (Fig. 6B, panel 4), indicating that the N-terminal domain of NL63-S does not interfere with CD13 binding as conferred by the central and C-terminal amino acids of 229E-S. The same observation was made for the converse chimera: the N-terminal domain of 229E-S did not interfere with hACE2 interaction by the central and C-terminal amino acids of NL63-S (chimera 229E-S-b) (Fig. 6B, panel 5). However, the hACE2 interaction was lost when the N-terminal and central sequences of NL63-S were exchanged for those of 229E-S (chimera NL63-S-1) (Fig. 6B, panel 3), this chimera did not gain any binding activity towards CD13, and the same observation was made for the converse construct (chimera 229E-S-a) (Fig. 6B, panel 6). Similarly, when only the central domain between both S-proteins was exchanged (chimeras NL63-S-3/229E-S-c), no binding to either CD13 or

hACE2 was observed (Fig. 6A). These results suggest that amino acids both in the central part and the C-terminal part of NL63-S and 229E-S are required for receptor recognition. As the C-terminal parts of the S1 domains of NL63- and 229E-S have the highest amino acid homology (72%), we speculated that receptor binding specificity might be mainly controlled by amino acids in the central domains, which exhibit an amino acid identity of 46% (Fig. 6A). In order to investigate which sequences in the central parts of NL63-S or 229E-S play a role in receptor recognition, we subdivided the central domain into several regions which were exchanged between NL63-S and 229E-S, resulting in chimeras 4 to 7 for NL63-S and d to g for 229E-S (Fig. 7A; normalization for comparable protein content is shown in B). Maybe most notably, replacement of NL63-S residues 510 to 549 by the corresponding sequences of 229E-S (chimera NL63-S-5) abolished the interaction with hACE2 and did not confer binding to CD13 (Fig. 7A). Similarly, exchange of residues 330 to 368 in 299E-S (chimera 229E-S-e) abrogated binding to CD13 and did not allow hACE2 engagement (Fig. 7A), suggesting an important role of the central domain in 229E- and NL63-S interactions with their receptors. In combination with the results obtained with the remaining chimeras (Fig. 7A), we conclude the following: for hACE2 recognition by NL63-S, amino acids 510 to 549 of the central part in combination with the C-terminal domain are required. CD13 binding by 229E-S is likewise dependent on the C-terminal domain and additionally requires amino acids 278 to 329 of the central domain. This is in contrast to published data, which identified amino acids 417 to 547 as a minimal CD13 binding domain by stepwise deletion mutagenesis (6, 7). In our hands, however, a 229E-S truncation comprising these residues did not bind CD13 in the FACS-based binding assay (Fig. 7, mutant 229E-S-h), thus further supporting a role of central sequences in receptor binding. Concerning the central domain, it is noteworthy that the amino acid alignment of both S-proteins contains three small stretches in which one S-protein lacks 3 to 5 amino acids present in the other one (motifs PQS, aa 310 to 312, and NFNE, aa 331 to 334 in 229E-S and motif SPGDS, aa 509 to 513, in NL63-S), which could alter the three-dimensional structure of the underlying protein. We therefore either deleted these motifs or exchanged them between NL63-S and 229E-S, followed by determination of receptor binding. However, we found that none of the chimeras was able to interact with either CD13 or hACE2 (data not shown), suggesting that insertion or deletion mutagenesis of the central region in either S-protein might severely affect the overall structure. In summary, the receptor binding domains of both NL63-S and 229E-S involve distinct parts located in their center and the C-terminal domains, but only extensive point mutagenesis in these regions might identify residues with a critical role in the hACE2 and CD13 interaction.

DISCUSSION

We have previously demonstrated that hCoV-NL63 engages the SARS-CoV receptor hACE2 for cellular entry (29). Here, we show that expression of hACE2 but not the cellular lectins DC-SIGN and DC-SIGNR allows for NL63-S-dependent entry into otherwise-nonpermissive cells, confirming that hACE2 fulfills the criteria of a bona fide receptor for hCoV-NL63. However, residues in hACE2 important for the interaction with SARS-S did not modulate NL63-S engagement of this receptor, and pseudotypes bearing NL63-S or SARS-S exhibited a differential dependence on low pH and protease cleavage for cellular entry, suggesting differences in SARS-S- and NL63-S-driven entry. Finally, mutagenic analyses of the highly related NL63-S and 229E-S proteins revealed that an N-terminal unique domain in NL63-S is dispensable for hACE2 binding, while sequences in the central and C-terminal regions of the S1 subunits of both NL63-S and 229E-S were required for binding to the cellular receptors hACE2 and CD13, respectively.

Within a previous study, we obtained evidence that the NL63-S protein binds to hACE2 and that hACE2 plays a key role in hCoV-NL63 entry (29). However, this study did not address whether hACE2 expression alone is sufficient to render otherwise-nonpermissive cells susceptible to NL63-S-dependent infection, which would provide formal proof of the receptor function of hACE2. We now show that exogenous expression of hACE2 on otherwise-nonpermissive BHK and HeLa cells (Fig. 1A and data not shown) renders these cell lines permissive, underlining that hACE2 is a functional receptor for NL63-S-mediated infection and that engagement of a coreceptor is most likely not required for entry. Nevertheless, a role of a ubiquitously expressed entry cofactor, which is conserved among species, can formally not be excluded. Expression of the cellular lectins DC-SIGN and DC-SIGNR slightly augmented NL63-S-dependent entry but was not sufficient to facilitate infection (Fig. 1B). These results match observations we and others had previously made for SARS-CoV (43, 70). However, lectin-mediated augmentation of NL63-S-driven entry was less efficient than SARS-S-driven infection, which might be due to subtle differences in the modification of the respective S proteins with high mannose carbohydrates, which are recognized by DC-SIGN and DC-SIGNR (19). Expression of DC-SIGN by skin dendritic cells and of DC-SIGNR by cells in the lung and small bowel (9, 34), where at least some cells are double positive for DC-SIGNR and hACE2 (9), suggests that these lectins could impact SARS-CoV spread. While lectin-mediated enhancement of SARS-CoV infection in vitro indicates that DC-SIGN/R might augment viral replication and disease development in infected patients, a recent study reported a protective role of homozygous DC-SIGNR in SARS-CoV infection (9). The functional consequences of the SARS-CoV interaction with DC-SIGN/R therefore require further analysis.

Mutagenic and structural analyses revealed several amino acid substitutions between hACE2 and ACE2 from rodents that affect interactions with SARS-S (38, 42). Particularly, a K353H exchange present in rat ACE2 relative to hACE2 was shown to prevent efficient SARS-S binding to this receptor (42). Similarly, mACE2, which also harbors the K353H exchange, interacts with SARS-S less efficiently than hACE2 (39); however, the responsible amino acid exchanges have not been mapped. Generally, the effects of these species-specific exchanges in ACE2 on interactions with SARS-S were most pronounced when binding of soluble SARS-S was examined, while their impact on infection by SARS-S-bearing pseudotypes was often relatively modest (42). Thus, introduction of K353H into hACE2 diminished pseudotype infection only 30% (42), and

a less effective receptor function of mACE2 relative to hACE2 was only observed when low levels of the receptors were expressed (39). We screened more than 40 ACE2 mutants for their ability to promote SARS-S- and NL63-S-driven entry. Mutations were introduced into hACE2 based on the known crystal structure of ACE2 (38). Only three of the variants analyzed exhibited alterations in the interaction with SARS-S. Mutation K353H reduced SARS-S-dependent entry as described previously (42). An even more pronounced reduction was observed upon introduction of the changes E145A, N149A, and D157A in hACE2 (Fig. 2B and C). These amino acids are not in direct contact with SARS-S (38), and it is currently unclear how they affect the interaction with SARS-S. Finally, exchange Y510A slightly augmented receptor function but not surface expression (Fig. 2), and it again needs to be clarified how this mutation modulates SARS-S entry. Notably, however, none of the above-discussed mutations altered interactions with NL63-S in a pseudotype infection system (Fig. 2B) or a cell-cell fusion assay (Fig. 2C), indicating that the three-dimensional structures of these hACE2 variants were not severely affected. The observation that these variants were used efficiently only by NL63-S but not by SARS-S suggests that both S-proteins might contact hACE2 differentially.

Cellular entry of SARS-CoV depends on the activity of cathepsin L, an endosomal cysteine protease that requires a low-pH environment for optimal activity (32, 54). This protein cleaves SARS-S at so-far-unknown sites and thereby triggers SARS-S-dependent membrane fusion. Hence, the observations that SARS-CoV entry can be blocked by agents that neutralize intracellular pH (28, 55, 70), like bafilomycin A1, reflect inhibition of protease activity and not abrogation of a pH stimulus required for triggering the membrane fusion activity of SARS-S (55), as initially suggested. Analysis of pH and cathepsin dependence of NL63-S-driven infection revealed that bafilomycin A1 (Fig. 3A) or the cysteine protease inhibitor E64c (Fig. 3B) reduce NL63-S-driven infection only moderately (53% and 83%, respectively), while both compounds efficiently diminish infection by SARS-S-bearing pseudotypes (97% and 99%, respectively). Our results obtained upon bafilomycin A1 treatment of target cells are in agreement with a recent report (32), while the effect observed upon protease inhibition differed to some extent from that previously documented (32). Thus, Huang and colleagues did not detect inhibition of NL63-S-dependent infection by the protease inhibitor E64d or by cathepsin L-specific inhibitors when pseudotypes were used (32). Nevertheless, they observed cell type-dependent inhibition of hCoV-NL63 replication by high doses of a cathepsin L inhibitor (32). The differences obtained with pseudotypes might be due to differences in the expression levels of ACE2 on target cells; Huang et al. used 293T cells overexpressing exogenous hACE2 (32), while we employed untransfected 293T cells that express low levels of endogenous hACE2. In any case, both studies hint at a reduced dependency of hCoV-NL63 entry on low pH and cathepsins compared to cellular entry of SARS-CoV, suggesting that both viruses evolved different strategies to exploit hACE2 for entry into target cells.

The S proteins of hCoV-NL63 and hCoV-229E share 56% sequence identity, yet both bind to different cellular receptors, CD13 and ACE2 (6, 7, 29). A potential explanation for this unexpected differential receptor usage is the presence of a unique 178-amino-acid domain at the N terminus of NL63-S. This domain is absent in 229E-S or in any other protein deposited in the database and might constitute an ACE2 binding domain (62). However, deletion of the unique domain in NL63-S did not abrogate the interaction with hACE2 and did not allow binding to CD13. Likewise, fusing this domain to the N terminus of 229E-S neither conferred binding to ACE2 nor abrogated interactions with CD13 (Fig. 4A), indicating that the unique domain does not constitute an ACE2 binding domain and does not mask a cryptic CD13 binding domain in NL63-S. This conclusion is further substantiated by the observation that a 229E-S chimera comprising the C-terminal sequences of NL63-S efficiently interacted with hACE2 but not CD13 (229E-S-b) (Fig. 6). Importantly, the unique domain was dispensable not only for binding of soluble NL63-S–IgG chimeras to hACE2 but also for NL6S-S-driven membrane fusion, suggesting that this portion of NL63-S is not essential for the function of fusion-competent NL63-S trimers (Fig. 4B). One has to take into account, however, that receptor binding and membrane fusion of NL63-S lacking the unique domain were moderately diminished compared to the wild-type protein. Reduced expression of NL63-SΔ unique constructs might account for these defects and would hint towards a contribution of the unique domain to proper folding of NL63-S. In fact, since a number of patient sera with neutralizing abilities bind to this region (L. van der Hoek and B. Berkhout, personal communication), further investigation is required to clarify the contribution of the unique domain to NL63-S structure and antigenicity.

Further deletions of N- and C-terminal portions of NL63-S revealed that the residues 232 to 684 are required for recognition of hACE2 (Fig. 5), and characterization of a variety of chimeras between NL63-S and 229E-S suggests that residues in both the central and the C-terminal part of the S1 subunits of the respective S proteins are required for specific recognition of their cellular receptors or for conservation of structures required for receptor binding (Fig. 6 and 7). These findings contrast with previous reports suggesting that residues 417 to 547 of 229E-S constitute a minimal receptor binding domain (6, 7). The reasons for this discrepancy are at present unclear; however, it should be noted that different experimental systems were employed to assess 229E-S interactions with CD13 (receptor binding of bacterially purified S-protein fragments [6, 7] versus S-Fc fusion proteins [present study]). In summary, our data suggest that neither 229E-S nor NL63-S harbors a linear high-affinity receptor binding site, as has been defined in SARS-S (65). In light of the complex interactions of 229E-S and NL63-S with their cognate cellular receptors and the observation that receptor binding by these S-proteins is easily perturbed, extensive point mutagenesis will be required to define key residues mediating these interactions. Ultimately, however, structural analyses will be necessary to elucidate the receptor interactions of 229E-S and NL63-S.

ACKNOWLEDGMENTS

We thank B. Fleckenstein and K. von der Mark for support. We acknowledge F. Neipel and T. Stamminger for providing pAB61 and pGal5-luc and pGAL4-VP16, respectively. We also thank J. D. Reeves for help with the cell cell-fusion system and T. Herdegen and A. Schulz for access to the luminometer.

This work was supported by SFB 466 (H.H., A.M., T.G., M.G., and S.P.), GK 1071 (C.C.), and the Mid-Atlantic Regional Center for Biodefense and Emerging Infectious Diseases (NIH U54 AI057168) (G.S.).

REFERENCES

1. **Arden, K. E., M. D. Nissen, T. P. Sloots, and I. M. Mackay.** 2005. New human coronavirus, HCoV-NL63, associated with severe lower respiratory tract disease in Australia. J. Med. Virol. **75:**455–462.
2. **Babcock, G. J., D. J. Esshaki, W. D. Thomas, Jr., and D. M. Ambrosino.** 2004. Amino acids 270 to 510 of the severe acute respiratory syndrome coronavirus spike protein are required for interaction with receptor. J. Virol. **78:**4552–4560.
3. **Baer, G. S., D. H. Ebert, C. J. Chung, A. H. Erickson, and T. S. Dermody.** 1999. Mutant cells selected during persistent reovirus infection do not express mature cathepsin L and do not support reovirus disassembly. J. Virol. **73:**9532–9543.
4. **Bastien, N., K. Anderson, L. Hart, P. Van Caeseele, K. Brandt, D. Milley, T. Hatchette, E. C. Weiss, and Y. Li.** 2005. Human coronavirus NL63 infection in Canada. J. Infect. Dis. **191:**503–506.
5. **Birkmann, A., K. Mahr, A. Ensser, S. Yaguboglu, F. Titgemeyer, B. Fleckenstein, and F. Neipel.** 2001. Cell surface heparan sulfate is a receptor for human herpesvirus 8 and interacts with envelope glycoprotein K8.1. J. Virol. **75:**11583–11593.
6. **Bonavia, A., B. D. Zelus, D. E. Wentworth, P. J. Talbot, and K. V. Holmes.** 2003. Identification of a receptor-binding domain of the spike glycoprotein of human coronavirus HCoV-229E. J. Virol. **77:**2530–2538.
7. **Breslin, J. J., I. Mork, M. K. Smith, L. K. Vogel, E. M. Hemmila, A. Bonavia, P. J. Talbot, H. Sjostrom, O. Noren, and K. V. Holmes.** 2003. Human coronavirus 229E: receptor binding domain and neutralization by soluble receptor at 37 degrees C. J. Virol. **77:**4435–4438.
8. **Chakraborti, S., P. Prabakaran, X. Xiao, and D. S. Dimitrov.** 2005. The SARS coronavirus S glycoprotein receptor binding domain: fine mapping and functional characterization. Virol. J. **2:**73.
9. **Chan, V. S., K. Y. Chan, Y. Chen, L. L. Poon, A. N. Cheung, B. Zheng, K. H. Chan, W. Mak, H. Y. Ngan, X. Xu, G. Screaton, P. K. Tam, J. M. Austyn, L. C. Chan, S. P. Yip, M. Peiris, U. S. Khoo, and C. L. Lin.** 2006. Homozygous L-SIGN (CLEC4M) plays a protective role in SARS coronavirus infection. Nat. Genet. **38:**38–46.
10. **Chandran, K., N. J. Sullivan, U. Felbor, S. P. Whelan, and J. M. Cunningham.** 2005. Endosomal proteolysis of the Ebola virus glycoprotein is necessary for infection. Science **308:**1643–1645.
11. **Chang, L. Y., B. L. Chiang, C. L. Kao, M. H. Wu, P. J. Chen, B. Berkhout, H. C. Yang, and L. M. Huang.** 2006. Lack of association between infection with a novel human coronavirus (HCoV), HCoV-NH, and Kawasaki disease in Taiwan. J. Infect. Dis. **193:**283–286.
12. **Connor, R. I., B. K. Chen, S. Choe, and N. R. Landau.** 1995. Vpr is required for efficient replication of human immunodeficiency virus type-1 in mononuclear phagocytes. Virology **206:**935–944.
13. **Danilczyk, U., U. Eriksson, M. A. Crackower, and J. M. Penninger.** 2003. A story of two ACEs. J. Mol. Med. **81:**227–234.
14. **Delmas, B., J. Gelfi, R. L'Haridon, L. K. Vogel, H. Sjostrom, O. Noren, and H. Laude.** 1992. Aminopeptidase N is a major receptor for the enteropathogenic coronavirus TGEV. Nature **357:**417–420.
15. **Ding, Y., L. He, Q. Zhang, Z. Huang, X. Che, J. Hou, H. Wang, H. Shen, L. Qiu, Z. Li, J. Geng, J. Cai, H. Han, X. Li, W. Kang, D. Weng, P. Liang, and S. Jiang.** 2004. Organ distribution of severe acute respiratory syndrome (SARS) associated coronavirus (SARS-CoV) in SARS patients: implications for pathogenesis and virus transmission pathways. J. Pathol. **203:**622–630.
16. **Ebert, D. H., S. A. Kopecky-Bromberg, and T. S. Dermody.** 2004. Cathepsin B is inhibited in mutant cells selected during persistent reovirus infection. J. Biol. Chem. **279:**3837–3851.
17. **Esper, F., E. D. Shapiro, C. Weibel, D. Ferguson, M. L. Landry, and J. S. Kahn.** 2005. Association between a novel human coronavirus and Kawasaki disease. J. Infect. Dis. **191:**499–502.
18. **Esper, F., C. Weibel, D. Ferguson, M. L. Landry, and J. S. Kahn.** 2005. Evidence of a novel human coronavirus that is associated with respiratory tract disease in infants and young children. J. Infect. Dis. **191:**492–498.
19. **Feinberg, H., D. A. Mitchell, K. Drickamer, and W. I. Weis.** 2001. Structural basis for selective recognition of oligosaccharides by DC-SIGN and DC-SIGNR. Science **294:**2163–2166.
20. **Fouchier, R. A., N. G. Hartwig, T. M. Bestebroer, B. Niemeyer, J. C. de Jong, J. H. Simon, and A. D. Osterhaus.** 2004. A previously undescribed coronavirus associated with respiratory disease in humans. Proc. Natl. Acad. Sci. USA **101:**6212–6216.
21. **Golden, J. W., J. A. Bahe, W. T. Lucas, M. L. Nibert, and L. A. Schiff.** 2004. Cathepsin S supports acid-independent infection by some reoviruses. J. Biol. Chem. **279:**8547–8557.
22. **Gramberg, T., H. Hofmann, P. Moller, P. F. Lalor, A. Marzi, M. Geier, M. Krumbiegel, T. Winkler, F. Kirchhoff, D. H. Adams, S. Becker, J. Munch, and S. Pöhlmann.** 2005. LSECtin interacts with filovirus glycoproteins and the spike protein of SARS coronavirus. Virology **340:**224–236.
23. **Gu, J., E. Gong, B. Zhang, J. Zheng, Z. Gao, Y. Zhong, W. Zou, J. Zhan, S. Wang, Z. Xie, H. Zhuang, B. Wu, H. Zhong, H. Shao, W. Fang, D. Gao, F. Pei, X. Li, Z. He, D. Xu, X. Shi, V. M. Anderson, and A. S. Leong.** 2005. Multiple organ infection and the pathogenesis of SARS. J. Exp. Med. **202:**415–424.
24. **Guan, Y., B. J. Zheng, Y. Q. He, X. L. Liu, Z. X. Zhuang, C. L. Cheung, S. W. Luo, P. H. Li, L. J. Zhang, Y. J. Guan, K. M. Butt, K. L. Wong, K. W. Chan, W. Lim, K. F. Shortridge, K. Y. Yuen, J. S. Peiris, and L. L. Poon.** 2003. Isolation and characterization of viruses related to the SARS coronavirus from animals in southern China. Science **302:**276–278.
25. **Hamming, I., W. Timens, M. L. Bulthuis, A. T. Lely, G. J. Navis, and H. van Goor.** 2004. Tissue distribution of ACE2 protein, the functional receptor for SARS coronavirus. A first step in understanding SARS pathogenesis. J. Pathol. **203:**631–637.
26. **He, J., S. Choe, R. Walker, P. Di Marzio, D. O. Morgan, and N. R. Landau.** 1995. Human immunodeficiency virus type 1 viral protein R (Vpr) arrests cells in the G_2 phase of the cell cycle by inhibiting $p34^{cdc2}$ activity. J. Virol. **69:**6705–6711.
27. **Hofmann, H., M. Geier, A. Marzi, M. Krumbiegel, M. Peipp, G. H. Fey, T. Gramberg, and S. Pöhlmann.** 2004. Susceptibility to SARS coronavirus S protein-driven infection correlates with expression of angiotensin converting enzyme 2 and infection can be blocked by soluble receptor. Biochem. Biophys. Res. Commun. **319:**1216–1221.
28. **Hofmann, H., K. Hattermann, A. Marzi, T. Gramberg, M. Geier, M. Krumbiegel, S. Kuate, K. Überla, M. Niedrig, and S. Pöhlmann.** 2004. S protein of severe acute respiratory syndrome-associated coronavirus mediates entry into hepatoma cell lines and is targeted by neutralizing antibodies in infected patients. J. Virol. **78:**6134–6142.
29. **Hofmann, H., K. Pyrc, L. van der Hoek, M. Geier, B. Berkhout, and S. Pöhlmann.** 2005. Human coronavirus NL63 employs the severe acute respiratory syndrome coronavirus receptor for cellular entry. Proc. Natl. Acad. Sci. USA **102:**7988–7993.
30. **Holmes, K. V.** 2001. Coronaviruses, p. 1187–1203. *In* D. M. Knipe et al. (ed.), Fields virology, 3rd ed. Lippincott, Williams, & Wilkins, Philadelphia, Pa.
31. **Holmes, K. V.** 2005. Structural biology. Adaptation of SARS coronavirus to humans. Science **309:**1822–1823.
32. **Huang, I. C., B. J. Bosch, F. Li, W. Li, K. H. Lee, S. Ghiran, N. Vasilieva, T. S. Dermody, S. C. Harrison, P. R. Dormitzer, M. Farzan, P. J. Rottier, and H. Choe.** 2006. SARS coronavirus, but not human coronavirus NL63, utilizes cathepsin L to infect ACE2-expressing cells. J. Biol. Chem. **281:**3198–3203.
33. **Imai, Y., K. Kuba, S. Rao, Y. Huan, F. Guo, B. Guan, P. Yang, R. Sarao, T. Wada, H. Leong-Poi, M. A. Crackower, A. Fukamizu, C. C. Hui, L. Hein, S. Uhlig, A. S. Slutsky, C. Jiang, and J. M. Penninger.** 2005. Angiotensin-converting enzyme 2 protects from severe acute lung failure. Nature **436:**112–116.
34. **Jeffers, S. A., S. M. Tusell, L. Gillim-Ross, E. M. Hemmila, J. E. Achenbach, G. J. Babcock, W. D. Thomas, Jr., L. B. Thackray, M. D. Young, R. J. Mason, D. M. Ambrosino, D. E. Wentworth, J. C. Demartini, and K. V. Holmes.** 2004. CD209L (L-SIGN) is a receptor for severe acute respiratory syndrome coronavirus. Proc. Natl. Acad. Sci. USA **101:**15748–15753.
35. **Kaiser, L., N. Regamey, H. Roiha, C. Deffernez, and U. Frey.** 2005. Human coronavirus NL63 associated with lower respiratory tract symptoms in early life. Pediatr. Infect. Dis. J. **24:**1015–1017.
36. **Kuba, K., Y. Imai, S. Rao, H. Gao, F. Guo, B. Guan, Y. Huan, P. Yang, Y. Zhang, W. Deng, L. Bao, B. Zhang, G. Liu, Z. Wang, M. Chappell, Y. Liu, D. Zheng, A. Leibbrandt, T. Wada, A. S. Slutsky, D. Liu, C. Qin, C. Jiang, and J. M. Penninger.** 2005. A crucial role of angiotensin converting enzyme 2 (ACE2) in SARS coronavirus-induced lung injury. Nat. Med. **11:**875–879.
37. **Lau, S. K., P. C. Woo, K. S. Li, Y. Huang, H. W. Tsoi, B. H. Wong, S. S. Wong, S. Y. Leung, K. H. Chan, and K. Y. Yuen.** 2005. Severe acute respiratory syndrome coronavirus-like virus in Chinese horseshoe bats. Proc. Natl. Acad. Sci. USA **102:**14040–14045.
38. **Li, F., W. Li, M. Farzan, and S. C. Harrison.** 2005. Structure of SARS coronavirus spike receptor-binding domain complexed with receptor. Science **309:**1864–1868.
39. **Li, W., T. C. Greenough, M. J. Moore, N. Vasilieva, M. Somasundaran, J. L. Sullivan, M. Farzan, and H. Choe.** 2004. Efficient replication of severe acute respiratory syndrome coronavirus in mouse cells is limited by murine angiotensin-converting enzyme 2. J. Virol. **78:**11429–11433.
40. **Li, W., M. J. Moore, N. Vasilieva, J. Sui, S. K. Wong, M. A. Berne, M. Somasundaran, J. L. Sullivan, K. Luzuriaga, T. C. Greenough, H. Choe, and M. Farzan.** 2003. Angiotensin-converting enzyme 2 is a functional receptor for the SARS coronavirus. Nature **426:**450–454.
41. **Li, W., Z. Shi, M. Yu, W. Ren, C. Smith, J. H. Epstein, H. Wang, G. Crameri, Z. Hu, H. Zhang, J. Zhang, J. McEachern, H. Field, P. Daszak, B. T. Eaton, S. Zhang, and L. F. Wang.** 2005. Bats are natural reservoirs of SARS-like coronaviruses. Science **310:**676–679.
42. **Li, W., C. Zhang, J. Sui, J. H. Kuhn, M. J. Moore, S. Luo, S. K. Wong, I. C. Huang, K. Xu, N. Vasilieva, A. Murakami, Y. He, W. A. Marasco, Y. Guan,**

H. Choe, and M. Farzan. 2005. Receptor and viral determinants of SARS-coronavirus adaptation to human ACE2. EMBO J. **24:**1634–1643.
43. **Marzi, A., T. Gramberg, G. Simmons, P. Moller, A. J. Rennekamp, M. Krumbiegel, M. Geier, J. Eisemann, N. Turza, B. Saunier, A. Steinkasserer, S. Becker, P. Bates, H. Hofmann, and S. Pöhlmann.** 2004. DC-SIGN and DC-SIGNR Interact with the glycoprotein of Marburg virus and the S protein of severe acute respiratory syndrome coronavirus. J. Virol. **78:**12090–12095.
44. **Matlin, K. S., H. Reggio, A. Helenius, and K. Simons.** 1982. Pathway of vesicular stomatitis virus entry leading to infection. J. Mol. Biol. **156:**609–631.
45. **McClure, M. O., M. Marsh, and R. A. Weiss.** 1988. Human immunodeficiency virus infection of CD4-bearing cells occurs by a pH-independent mechanism. EMBO J. **7:**513–518.
46. **McClure, M. O., M. A. Sommerfelt, M. Marsh, and R. A. Weiss.** 1990. The pH independence of mammalian retrovirus infection. J. Gen. Virol. **71:**767–773.
47. **Moes, E., L. Vijgen, E. Keyaerts, K. Zlateva, S. Li, P. Maes, K. Pyrc, B. Berkhout, L. van der Hoek, and M. Van Ranst.** 2005. A novel pancoronavirus RT-PCR assay: frequent detection of human coronavirus NL63 in children hospitalized with respiratory tract infections in Belgium. BMC Infect. Dis. **5:**6.
48. **Nie, Y., P. Wang, X. Shi, G. Wang, J. Chen, A. Zheng, W. Wang, Z. Wang, X. Qu, M. Luo, L. Tan, X. Song, X. Yin, J. Chen, M. Ding, and H. Deng.** 2004. Highly infectious SARS-CoV pseudotyped virus reveals the cell tropism and its correlation with receptor expression. Biochem. Biophys. Res. Commun. **321:**994–1000.
49. **Niwa, H., K. Yamamura, and J. Miyazaki.** 1991. Efficient selection for high-expression transfectants with a novel eukaryotic vector. Gene **108:**193–199.
50. **Peiris, J. S., Y. Guan, and K. Y. Yuen.** 2004. Severe acute respiratory syndrome. Nat. Med. **10:**88–97.
51. **Peiris, J. S., K. Y. Yuen, A. D. Osterhaus, and K. Stohr.** 2003. The severe acute respiratory syndrome. N. Engl. J. Med. **349:**2431–2441.
52. **Pyrc, K., M. F. Jebbink, B. Berkhout, and L. van der Hoek.** 2004. Genome structure and transcriptional regulation of human coronavirus NL63. Virol. J. **1:**7.
53. **Shimizu, C., H. Shike, S. C. Baker, F. Garcia, L. van der Hoek, T. W. Kuijpers, S. L. Reed, A. H. Rowley, S. T. Shulman, H. K. Talbot, J. V. Williams, and J. C. Burns.** 2005. Human coronavirus NL63 is not detected in the respiratory tracts of children with acute Kawasaki disease. J. Infect. Dis. **192:**1767–1771.
54. **Simmons, G., D. N. Gosalia, A. J. Rennekamp, J. D. Reeves, S. L. Diamond, and P. Bates.** 2005. Inhibitors of cathepsin L prevent severe acute respiratory syndrome coronavirus entry. Proc. Natl. Acad. Sci. USA **102:**11876–11881.
55. **Simmons, G., J. D. Reeves, A. J. Rennekamp, S. M. Amberg, A. J. Piefer, and P. Bates.** 2004. Characterization of severe acute respiratory syndrome-associated coronavirus (SARS-CoV) spike glycoprotein-mediated viral entry. Proc. Natl. Acad. Sci. USA **101:**4240–4245.
56. **Smith, A. E., and A. Helenius.** 2004. How viruses enter animal cells. Science **304:**237–242.
57. **Stadler, K., V. Masignani, M. Eickmann, S. Becker, S. Abrignani, H. D. Klenk, and R. Rappuoli.** 2003. SARS: beginning to understand a new virus. Nat. Rev. Microbiol. **1:**209–218.
58. **Stadler, K., and R. Rappuoli.** 2005. SARS: understanding the virus and development of rational therapy. Curr. Mol. Med. **5:**677–697.
59. **Stamminger, T., M. Gstaiger, K. Weinzierl, K. Lorz, M. Winkler, and W. Schaffner.** 2002. Open reading frame UL26 of human cytomegalovirus encodes a novel tegument protein that contains a strong transcriptional activation domain. J. Virol. **76:**4836–4847.
60. **Suzuki, A., M. Okamoto, A. Ohmi, O. Watanabe, S. Miyabayashi, and H. Nishimura.** 2005. Detection of human coronavirus-NL63 in children in Japan. Pediatr. Infect. Dis. J. **24:**645–646.
61. **Vabret, A., T. Mourez, J. Dina, L. van der Hoek, S. Gouarin, J. Petitjean, J. Brouard, and F. Freymuth.** 2005. Human coronavirus NL63, France. Emerg. Infect. Dis. **11:**1225–1229.
62. **van der Hoek, L., K. Pyrc, M. F. Jebbink, W. Vermeulen-Oost, R. J. Berkhout, K. C. Wolthers, P. M. Wertheim-van Dillen, J. Kaandorp, J. Spaargaren, and B. Berkhout.** 2004. Identification of a new human coronavirus. Nat. Med. **10:**368–373.
63. **van der Hoek, L., K. Sure, G. Ihorst, A. Stang, K. Pyrc, M. F. Jebbink, G. Petersen, J. Forster, B. Berkhout, and K. Überla.** 2005. Croup is associated with the novel coronavirus NL63. PLoS Med. **2:**e240.
64. **Wang, P., J. Chen, A. Zheng, Y. Nie, X. Shi, W. Wang, G. Wang, M. Luo, H. Liu, L. Tan, X. Song, Z. Wang, X. Yin, X. Qu, X. Wang, T. Qing, M. Ding, and H. Deng.** 2004. Expression cloning of functional receptor used by SARS coronavirus. Biochem. Biophys. Res. Commun. **315:**439–444.
65. **Wong, S. K., W. Li, M. J. Moore, H. Choe, and M. Farzan.** 2004. A 193-amino acid fragment of the SARS coronavirus S protein efficiently binds angiotensin-converting enzyme 2. J. Biol. Chem. **279:**3197–3201.
66. **Woo, P. C., S. K. Lau, C. M. Chu, K. H. Chan, H. W. Tsoi, Y. Huang, B. H. Wong, R. W. Poon, J. J. Cai, W. K. Luk, L. L. Poon, S. S. Wong, Y. Guan, J. S. Peiris, and K. Y. Yuen.** 2005. Characterization and complete genome sequence of a novel coronavirus, coronavirus HKU1, from patients with pneumonia. J. Virol. **79:**884–895.
67. **Woo, P. C., S. K. Lau, H. W. Tsoi, Y. Huang, R. W. Poon, C. M. Chu, R. A. Lee, W. K. Luk, G. K. Wong, B. H. Wong, V. C. Cheng, B. S. Tang, A. K. Wu, R. W. Yung, H. Chen, Y. Guan, K. H. Chan, and K. Y. Yuen.** 2005. Clinical and molecular epidemiological features of coronavirus HKU1-associated community-acquired pneumonia. J. Infect. Dis. **192:**1898–1907.
68. **Wu, L., T. D. Martin, M. Carrington, and V. N. Kewalramani.** 2004. Raji B cells, misidentified as THP-1 cells, stimulate DC-SIGN-mediated HIV transmission. Virology **318:**17–23.
69. **Xiao, X., S. Chakraborti, A. S. Dimitrov, K. Gramatikoff, and D. S. Dimitrov.** 2003. The SARS-CoV S glycoprotein: expression and functional characterization. Biochem. Biophys. Res. Commun. **312:**1159–1164.
70. **Yang, Z. Y., Y. Huang, L. Ganesh, K. Leung, W. P. Kong, O. Schwartz, K. Subbarao, and G. J. Nabel.** 2004. pH-dependent entry of severe acute respiratory syndrome coronavirus is mediated by the spike glycoprotein and enhanced by dendritic cell transfer through DC-SIGN. J. Virol. **78:**5642–5650.
71. **Yeager, C. L., R. A. Ashmun, R. K. Williams, C. B. Cardellichio, L. H. Shapiro, A. T. Look, and K. V. Holmes.** 1992. Human aminopeptidase N is a receptor for human coronavirus 229E. Nature **357:**420–422.